Time-dependent close-coupling calculations for the electron-impact ionization of carbon and neon

M. S. Pindzola, J. Colgan, and F. Robicheaux
Department of Physics, Auburn University, Auburn, Alabama 36849

D. C. Griffin
Department of Physics, Rollins College, Winter Park, Florida 32789
(Received 26 May 2000; published 11 September 2000)

A time-dependent close-coupling method is used to calculate the electron-impact ionization cross section for the outer $2p$ subshell of both carbon and neon atoms. The inner $1s$ and $2s$ subshells are treated using pseudopotentials, while interaction with the remaining $2p$ core electrons is handled in a configuration-average approximation. When the time-dependent ionization cross section for the $2p$ subshell of carbon is combined with distorted-wave ionization cross sections for the $2s$ subshell, the resulting total cross section is in reasonable agreement with previous experimental measurements. However, when the time-dependent ionization cross section for the $2p$ subshell of neon is combined with distorted-wave ionization cross sections for the $2s$ subshell, the resulting total cross section is substantially higher than all previous experimental measurements. Further LS term-dependent distorted-wave ionization cross sections for the $2p$ subshell of neon suggest the need for extending the time-dependent close-coupling method to include a full Hartree-Fock interaction with the remaining $2p$ core electrons.

PACS number(s): 34.80.Kw

I. INTRODUCTION

The electron-impact single ionization of an arbitrary atom or ion remains a formidable theoretical and computational challenge. The basic direct ''knockout'' ionization process involves two escaping electrons in a long-range Coulomb field; that is the quantal three-body problem. The direct process is the dominant ionization mechanism for most atoms and low-charged positive ions. Additional indirect ionization processes, like excitation-autoionization, become relatively large for multiply charged positive ions with a small number of valence electrons outside closed subshells.

One of the most widely used fully quantal methods for treating direct ionization of arbitrary atoms and ions has been the application of first-order perturbation theory using distorted waves [1,2]. However, little work has been done on extending the method to include higher-order perturbative effects to ascertain the overall accuracy of the first-order results. Recently, fully quantal nonperturbative methods have been developed and applied to the direct ionization of one and two electron valence subshell atoms and ions. For the first time the accuracy of the first-order distorted-wave method, as well as experimental measurements, can be accurately assessed.

Electron ionization cross sections for hydrogen calculated using converged close coupling [3], hyperspherical close coupling [4], R-matrix pseudostates [5], and the time-dependent close-coupling [6] method are all in excellent agreement with experimental measurements [7], and about 15% lower than distorted-wave predictions [6]. Electron ionization cross sections for helium calculated using converged close coupling [8], R-matrix pseudostates [9], and the time-dependent close-coupling [10] method are again all in excellent agreement with experimental measurements [11], and about 10% lower than distorted-wave predictions [10]. Nonperturbative calculations for the direct ionization cross section of low-charged positive ions in the Li [12–19] and Na [20,21] isoelectronic sequences have revealed that distorted-wave predictions for the $2s$ and $3s$ subshells are reasonably accurate for ions with a charge of $3+$ or higher.

In this paper we extend the time-dependent close-coupling method to calculate the direct electron-impact ionization of the outer subshell of any atom or ion. The inner subshells are treated using pseudopotentials, while interaction with the remaining core electrons of the outer subshell is handled in a configuration-average approximation. We carry out nonperturbative time-dependent close-coupling calculations for the open-shell ground configuration $1s^2 2s^2 2p^2$ of neutral carbon and the closed-shell ground configuration $1s^2 2s^2 2p^6$ of neutral neon. We compare the nonperturbative close-coupling results for direct ionization of the $2p$ subshell with perturbative distorted-wave predictions. We then combine the close-coupling outer subshell results with distorted-wave ionization cross sections for the inner subshells to compare with previous experimental measurements. Although theory and experiment are in reasonable agreement for the single ionization of carbon, theory is substantially higher than experiment for the single ionization of neon. Further LS term-dependent distorted-wave calculations for the ionization of the $2p$ outer subshell of neon suggest the need for a further extension of the time-dependent close-coupling method to include a full Hartree-Fock interaction with the remaining $2p$ core electrons. The time-independent distorted-wave and time-dependent close-coupling methods are presented in Sec. II, electron-impact single-ionization cross sections for carbon and neon are presented in Sec. III, and a brief summary is found in Sec. IV.

II. THEORY

A. Time-independent distorted-wave method

The configuration-average distorted-wave expression for the direct ionization cross section of the $(n_t l_t)^{w_t}$ subshell of any atom is given by [22]

$$\sigma = \frac{16 w_t}{k_i^3} \int_0^E \frac{d(k_e^2/2)}{k_e k_f} \sum_{l_i, l_e, l_f} (2l_i+1)(2l_e+1) \times (2l_f+1) \mathcal{P}(l_i, l_e, l_f, k_i, k_e, k_f), \quad (1)$$

where the linear momenta (k_i, k_e, k_f) and the angular momentum quantum numbers (l_i, l_e, l_f) correspond to the incoming, ejected, and outgoing electrons, respectively. The total energy $E = (k_i^2/2) - I = (k_e^2/2) + (k_f^2/2)$, and I is the subshell ionization energy. The first-order scattering probability is given by [22]

$$\mathcal{P}(l_i, l_e, l_f, k_i, k_e, k_f) = \sum_{\lambda} A^{\lambda}_{l_i, l_e, l_f} [R^{\lambda}(k_e l_e, k_f l_f, n_t l_t, k_i l_i)]^2 \quad (2)$$

$$+ \sum_{\lambda'} B^{\lambda'}_{l_i, l_e, l_f} [R^{\lambda'}(k_f l_f, k_e l_e, n_t l_t, k_i l_i)]^2 \quad (3)$$

$$+ \sum_{\lambda} \sum_{\lambda'} C^{\lambda, \lambda'}_{l_i, l_e, l_f} R^{\lambda}(k_e l_e, k_f l_f, n_t l_t, k_i l_i) \times R^{\lambda'}(k_f l_f, k_e l_e, n_t l_t, k_i l_i), \quad (4)$$

where the angular coefficients A, B, and C may be expressed in terms of standard $3-j$ and $6-j$ symbols, and the R^{λ} are standard radial Slater integrals.

The radial distorted waves $P_{kl}(r)$ needed to evaluate the Slater integrals are solutions to a radial Schrödinger equation given by

$$\left(h(r) - \frac{k^2}{2} \right) P_{kl}(r) = 0, \quad (5)$$

where

$$h(r) = -\frac{1}{2} \frac{d^2}{dr^2} + \frac{l(l+1)}{2r^2} - \frac{Z}{r} + V_D(r) + V_X(r), \quad (6)$$

and Z is the atomic number. The direct V_D potential is given by

$$V_D(r) = \sum_u w_u \int_0^{\infty} \frac{P^2_{n_u l_u}(r')}{\max(r', r)} dr', \quad (7)$$

where $P_{n_u l_u}(r)$ are bound Hartree-Fock orbitals. The local exchange V_X potential is constructed using bound orbital radial probability densities. The incident and scattered electron continuum orbitals are evaluated in a V^N potential, while the ejected continuum orbital is calculated in a V^{N-1} potential, where $N = \Sigma_u w_u$ is the number of target electrons. This, in intercombination with the interchange of the potentials for the ejected and scattered electrons in the exchange terms of the scattering probability, eliminates one-particle potential terms [1]. The continuum normalization for all distorted waves is one times a sine function.

B. Time-dependent close-coupling method

The configuration-average time-dependent close-coupling expression for the direct ionization of the $(n_t l_t)^{w_t}$ subshell of any atom is given by [6,10]

$$\sigma = \frac{w_t \pi}{4(2l_t+1)k_i^2} \int_0^E \frac{d(k_e^2/2)}{k_e k_f} \sum_{l_i, l_e, l_f} \sum_{L,S} (2L+1) \times (2S+1) \mathcal{P}(l_i, l_e, l_f, L, S, k_i, k_e, k_f), \quad (8)$$

where L is the angular momentum quantum number obtained by coupling l_t and l_i (or l_e and l_f), and S is the spin momentum quantum number obtained by coupling two spin-$\frac{1}{2}$ electrons. The scattering probability is given by

$$\mathcal{P}(l_i, l_e, l_f, L, S, k_i, k_e, k_f) = \left| \int_0^{\infty} dr_1 \int_0^{\infty} dr_2 \overline{P}_{k_e l_e}(r_1) \overline{P}_{k_f l_f}(r_2) \times P^{LS}_{l_i l_e l_f}(r_1, r_2, t=T) \right|^2. \quad (9)$$

The two-dimensional radial wave functions $P^{LS}_{l_0 l_1 l_2}(r_1, r_2, t)$ are solutions to the time-dependent radial Schrödinger equation given by

$$i \frac{\partial P^{LS}_{l_0 l_1 l_2}(r_1, r_2, t)}{\partial t} = T_{l_1 l_2}(r_1, r_2) P^{LS}_{l_0 l_1 l_2}(r_1, r_2, t) + \sum_{l_1', l_2'} U^L_{l_1 l_2, l_1' l_2'}(r_1, r_2) P^{LS}_{l_0 l_1' l_2'}(r_1, r_2, t), \quad (10)$$

where

$$T_{l_1 l_2}(r_1, r_2) = -\frac{1}{2} \frac{\partial^2}{\partial r_1^2} - \frac{1}{2} \frac{\partial^2}{\partial r_2^2} + \frac{l_1(l_1+1)}{2r_1^2} + \frac{l_2(l_2+1)}{2r_2^2} - \frac{Z}{r_1} + V_D(r_1) + V_X(r_1) - \frac{Z}{r_2} + V_D(r_2) + V_X(r_2), \quad (11)$$

and the coupling operator is given by

$$U^L_{l_1 l_2, l_1' l_2'}(r_1, r_2) = (-1)^{L + l_2 + l_2'} \sqrt{(2l_1+1)(2l_1'+1)(2l_2+1)(2l_2'+1)} \times \sum_{\lambda} \frac{r_<^{\lambda}}{r_>^{\lambda+1}} \begin{pmatrix} l_1 & \lambda & l_1' \\ 0 & 0 & 0 \end{pmatrix} \begin{pmatrix} l_2 & \lambda & l_2' \\ 0 & 0 & 0 \end{pmatrix} \begin{Bmatrix} L & l_2' & l_1' \\ \lambda & l_1 & l_2 \end{Bmatrix}. \quad (12)$$

The initial condition for the solution of the time-dependent radial Schrödinger equation is given by

$$P^{LS}_{l_0 l_1 l_2}(r_1,r_2,t=0)=\sqrt{\frac{1}{2}}(\delta_{l_0,l_1}G_{k_1 l_1}(r_1)\delta_{l_t,l_2}\overline{P}_{n_t l_t}(r_2) + (-1)^S\delta_{l_t,l_1}\overline{P}_{n_t l_t}(r_1)\delta_{l_0,l_2}G_{k_2 l_2}(r_2)), \tag{13}$$

where $G_{kl}(r)$ is a radial wave packet and the factor $(-1)^S$ assures overall antisymmetry for the two-dimensional radial wave function. The radial wave function at a time $t=T$, following the collision, is obtained by propagating the time-dependent close-coupling equations on a two-dimensional finite lattice. The two-electron wave functions fully describe the correlation between the ejected and scattered electrons at all times following the collision. This exact nonperturbative treatment of the quantal three-body problem is what is missing in the approximate perturbative distorted-wave method described in Sec. II A.

The bound $\overline{P}_{nl}(r)$ and continuum $\overline{P}_{kl}(r)$ radial orbitals needed in Eqs. (9) and (13) are obtained by diagonalization of the Hamiltonian $h(r)$ of Eq. (6) on a one-dimensional finite lattice. The direct V_D and local exchange V_X potentials are constructed as pseudopotentials in which the inner nodes of the valence Hartree-Fock orbitals are removed in a smooth manner. This prevents unphysical excitation of filled subshells during time propagation of the close-coupled equations [14].

C. Branching ratios for LS term-selective ionization

Once configuration-averaged ionization cross sections are calculated with either the distorted-wave or close-coupling methods, individual $L_iS_i \rightarrow L_fS_f$ term-selective ionization cross sections may be easily obtained using the appropriate branching ratio [23]. For transitions

$$(n_t l_t)^{w_t} L_i S_i \rightarrow (n_t l_t)^{w_t-1} L_f S_f, \tag{14}$$

in which all the remaining inactive subshells are closed, the branching ratio is given by

$$B_{i\rightarrow f}=[c(l_t^{w_t-1}\ \ L_fS_f|\}l_t^{w_t}L_iS_i)]^2, \tag{15}$$

where c is a coefficient of fractional parentage. For transitions

$$((n_t l_t)^{w_t}L_tS_t(n_u l_u)^{w_u}L_uS_u)L_iS_i \rightarrow ((n_t l_t)^{w_t-1}L_t'S_t'(n_u l_u)^{w_u}L_uS_u)L_fS_f, \tag{16}$$

in which all the remaining inactive subshells are closed, the branching ratio is given by

$$B_{i\rightarrow f}=(2L_t+1)(2S_t+1)(2L_f+1)(2S_f+1) \times[c(l_t^{w_t-1}L_t'S_t'|\}l_t^{w_t}L_tS_t)]^2 \times\begin{Bmatrix} l_t & L_t' & L_t \\ L_u & L_i & L_f\end{Bmatrix}^2\begin{Bmatrix} 1/2 & S_t' & S_t \\ S_u & S_i & S_f\end{Bmatrix}^2. \tag{17}$$

TABLE I. Partial ionization cross sections (Mb) for carbon at three incident electron energies (l_i is the incident angular momentum). The time-dependent close-coupling (CC) calculations ''topped up'' with the time-independent distorted-wave (DW) results for $l_i=7-30$ to give a total ionization cross section. (1.0 Mb $=1.0\times10^{-18}$ cm^2).

Incident energy	40 eV		70 eV		100 eV	
l_i	CC	DW	CC	DW	CC	DW
0	4.18	4.55	3.79	3.74	2.84	2.84
1	17.80	31.28	11.84	15.37	8.33	8.80
2	14.97	26.85	12.08	15.93	8.84	9.94
3	31.39	44.41	22.13	25.20	15.06	14.93
4	26.94	35.38	22.98	26.34	17.03	17.34
5	21.81	26.61	22.18	24.71	17.76	18.03
6	18.31	19.66	21.40	22.17	18.33	17.66
0–6	135.40	188.74	116.40	133.46	88.19	89.54
7–30	-	41.02	-	86.27	-	98.55
Total Cross section	176.42	229.76	202.67	219.73	186.74	188.09

III. RESULTS

A. Electron scattering from carbon

Partial-wave ionization cross sections for electron scattering from the outer $2p$ subshell of carbon, calculated using the time-dependent close-coupling and time-independent distorted-wave methods, are presented in Table I. Both configuration-averaged calculations use an experimental ionization potential of 10.66 eV [24]. We find that, for most cases, the distorted-wave results are higher than the close-coupling results for each partial wave, resulting in a higher distorted-wave total cross section compared to the close-coupling total cross section at each incident electron energy.

The time-dependent close-coupling equations for the two-electron radial wave functions are solved on a numerical lattice with 250 points in each radial direction from 0 to 50 a.u., spanned by a uniform mesh spacing $\Delta r=0.20$ a.u. The total time propagation of the radial wave functions is determined by the convergence of the collision probabilities; in general, shorter times are needed for larger incident electron energies. The number of $(l_1 l_2)$ coupled channels ranges from four for $L=0$ to 24 for $L=6$. Time-independent distorted-wave calculations were also carried out for electron ionization of the $2s$ subshell of carbon at a configuration-average ionization potential of 18.0 eV.

Individual LS term-selective ionization cross sections may be easily obtained by multiplying the configuration-average ionization cross sections by the appropriate branching ratio [see Eqs. (15) and (17)] and ionization potential scaling factor determined using experimental energies [24]. Thus the $1s^22s^22p^2\ ^3P\rightarrow 1s^22s^22p\ ^2P$ cross section is obtained by multiplying the $1s^22s^22p^2\rightarrow 1s^22s^22p$ cross section by a branching ratio of 1 and by an ionization potential scaling factor of 10.66 eV divided by 11.26 eV. The $1s^22s^22p^2\ ^3P\rightarrow 1s^22s2p^2\ ^4P$ cross section is obtained by multiplying the $1s^22s^22p^2\rightarrow 1s^22s2p^2$ cross section by a

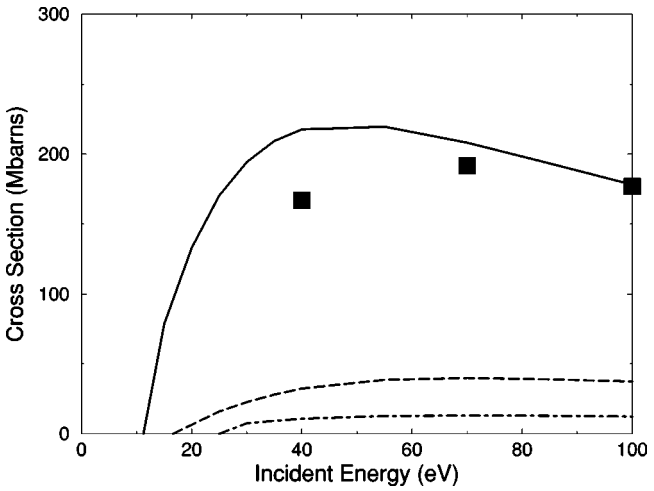

FIG. 1. Individual LS term-specific electron-impact ionization cross sections for carbon. Solid squares: time-dependent close-coupling calculations for $1s^2 2s^2 2p^2(^3P) \rightarrow 1s^2 2s^2 2p(^2P)$. Solid line: distorted-wave calculations for the $1s^2 2s^2 2p^2(^3P) \rightarrow 1s^2 2s^2 2p(^2P)$ cross section. Dashed line: distorted-wave calculations for the $1s^2 2s^2 2p^2(^3P) \rightarrow 1s^2 2s 2p^2(^4P)$ cross section. Dot-dashed line: distorted-wave calculations for the $1s^2 2s^2 2p^2(^3P) \rightarrow 1s^2 2s 2p^2(^2P)$ cross section. (1.0 Mb $= 1.0 \times 10^{-18}$ cm^2.)

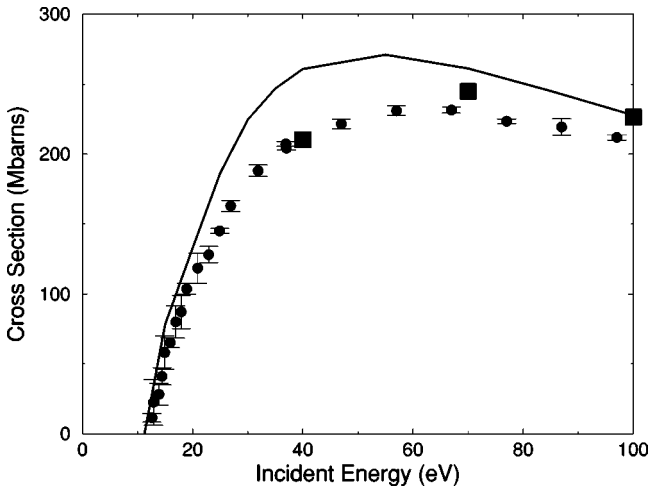

FIG. 2. Total electron-impact ionization cross section for carbon. Solid squares: time-dependent close-coupling calculations for $1s^2 2s^2 2p^2(^3P) \rightarrow 1s^2 2s^2 2p(^2P)$ combined with distorted-wave calculations for $1s^2 2s^2 2p^2(^3P) \rightarrow 1s^2 2s 2p^2(^{2,4}P)$. Solid line: time-independent distorted-wave calculations for $1s^2 2s^2 2p^2(^3P) \rightarrow 1s^2 2s^2 2p(^2P)$ and $1s^2 2s^2 2p^2(^3P) \rightarrow 1s^2 2s 2p^2(^{2,4}P)$. Solid circles: experimental points of Ref. [25]. (1.0 Mb $= 1.0 \times 10^{-18}$ cm^2.)

branching ratio of $\frac{2}{3}$ and by an ionization potential scaling factor of 18.0 eV divided by 16.6 eV, while the $1s^2 2s^2 2p^2\ ^3P \rightarrow 1s^2 2s 2p^2\ ^2P$ cross section is obtained by multiplying the same $1s^2 2s^2 2p^2 \rightarrow 1s^2 2s 2p^2$ cross section by a branching ratio of $\frac{1}{3}$ and by an ionization potential scaling factor of 18.0 eV divided by 25.0 eV.

The three individual LS term-selective cross sections resulting in single ionization of the $1s^2 2s^2 2p^2\ ^3P$ ground state of carbon are presented in Fig. 1. The solid squares are time-dependent close-coupling results, while the lines are time-independent distorted-wave results. The close-coupling results are ''topped up'' at the higher angular momentum ($l_0 \geqslant 7$) using distorted-wave cross sections. The difference in the close-coupling and distorted-wave results for the ionization of the $2p$ subshell is found to decrease slowly in moving to higher incident energies. Although not shown, LS term-selective cross sections from the $1s^2 2s^2 2p^2\ ^1D$ and $1s^2 2s^2 2p^2\ ^1S$ excited states may also be easily obtained from the branching ratio formulas. We checked the validity of using an ionization potential scaling factor by carrying out distorted-wave calculations at both the experimental ^3P term energy of 11.26 eV and the experimental configuration-average energy of 10.66 eV, and found that 0.95 worked well at all incident energies except those very close to threshold.

Total ionization cross sections for electron scattering from carbon at low incident energies are presented in Fig. 2. The solid circles with error bars are the experimental measurements of Brook *et al* [25]. An examination of the measurements near the lowest energy threshold indicates that ionization is almost completely from the $1s^2 2s^2 2p^2\ ^3P$ term, and not from a population blend over all the LS terms of the $1s^2 2s^2 2p^2$ ground configuration. Thus we add together the $1s^2 2s^2 2p^2\ ^3P$ ionization cross sections found in Fig. 1 to compare with experiment. We note that the configuration-averaged total cross section is equal to the cross section obtained from summing over all final states, apart from the energy scaling factors discussed previously. At the peak of the total ionization cross section the distorted-wave results are from 15% to 20% higher than experiment, while the close-coupling–distorted-wave hybrid results are almost that much lower and in much better agreement. We also calculated indirect ionization contributions coming from $2s \rightarrow 3s,3p,3d,4s,4p,4d$ excitation-autoionization, and found that the contribution has a maximum of 30 Mb at 20 eV, but then falls to 14 Mb near the peak at 60 eV. Therefore, even with an additional 5% increase in the total ionization cross section at its peak, the theoretical predictions including the nonperturbative close-coupling results for the $2p$ subshell are still in reasonable agreement with experiment for carbon.

B. Electron scattering from neon

Partial-wave ionization cross sections for electron scattering from the outer $2p$ subshell of neon, calculated using the time-dependent close-coupling and time-independent distorted-wave methods, are presented in Table II. Both configuration-averaged calculations use an experimental ionization potential of 21.56 eV [24]. The distorted-wave cross sections are generally higher than the time-dependent close-coupling cross sections, except for the lowest partial waves, so that the total cross section calculated using the distorted-wave and close-coupling methods are in close agreement.

The time-dependent close-coupling equations for the two-electron radial wave functions are solved on a numerical lattice with 250 points in each radial direction from 0 to 50 a.u., spanned by a uniform mesh spacing $\Delta r = 0.20$ a.u. The number of $(l_1 l_2)$ coupled channels ranges from four for $L = 0$ to

TABLE II. Partial ionization cross sections (Mb) for neon at three incident electron energies (l_i is the incident angular momentum). The time-dependent close-coupling (CC) calculations are ''topped up'' with the configuration-average distorted-wave (DW) results for $l_i=7-30$ to give the total ionization cross section. ($1.0\ \text{Mb}=1.0\times10^{-18}\ \text{cm}^2$).

Incident energy	100 eV		150 eV		200 eV	
l_i	CC	DW	CC	DW	CC	DW
0	2.10	1.79	1.90	1.61	1.63	1.39
1	11.33	10.31	8.42	7.24	6.60	5.15
2	8.59	6.29	7.34	6.14	6.10	4.95
3	12.80	16.27	11.01	11.88	8.91	8.36
4	10.31	13.18	9.96	11.51	8.65	9.05
5	8.39	10.61	8.92	10.53	8.16	8.95
6	7.26	8.36	8.26	9.33	7.88	8.48
0–6	60.78	66.81	55.81	58.24	47.93	46.33
7–30	-	21.20	-	35.94	-	43.31
Total Cross section	81.98	88.01	91.75	94.18	91.24	89.64

24 for $L=6$. Time-independent distorted-wave calculations were also carried out for electron ionization of the 2s subshell of neon at a configuration-averaged ionization potential of 49.3 eV. We note that due to the closed shell nature of the ground state of neon, that individual LS term-selective ionization cross sections are identical to the configuration-averaged cross sections.

Total ionization cross sections for electron scattering from neon at low incident energies are presented in Fig. 3. The solid circles with error bars are the experimental measurements of Krishnakumar and Srivastava [26]. This experiment agrees well with earlier experimental results [27] for neon, as well as recent low-energy results [28]. The solid squares are close-coupling results for $2p$ subshell ionization combined with distorted-wave results for $2s$ subshell ionization. They are in good agreement with the sum of distorted-wave calculations for both the $2p$ and $2s$ subshells, as indicated by the solid line. However, both total cross-section results are 25% higher than experiment at the peak of the cross section. We also calculated indirect ionization contributions coming from $2s\rightarrow3s,3p,3d,4s,4p,4d$ excitation-autoionization, and found a negligible contribution of only 1.2 Mb at 60 eV. Therefore, in contrast with the findings for carbon, the theoretical predictions including nonperturbative close-coupling results for the $2p$ subshell are substantially higher than experiment for neon.

Previous perturbative distorted-wave studies of the electron ionization of the outer closed subshell of argon [29,30] and the electron ionization of the inner closed subshells of rare-gas ions [31] have found that certain ejected electron continuua are completely misrepresented by a configuration-averaged scattering potential. In particular, these studies suggest that the dipole allowed $2p^6\ ^1S\rightarrow2p^5kd\ ^1P$ excitation contribution to the outer closed subshell ionization cross section for neon may show LS term-dependent effects. Thus we

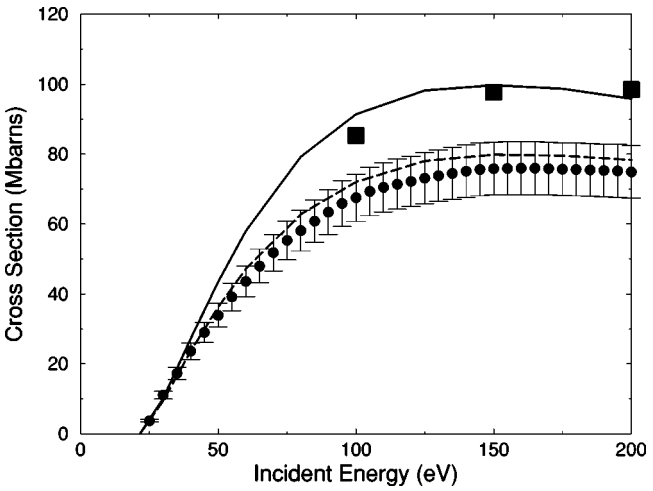

FIG. 3. Total electron-impact ionization cross section for neon. Solid squares: time-dependent close-coupling calculations for $1s^22s^22p^6\rightarrow1s^22s^22p^5$ combined with distorted-wave calculations for $1s^22s^22p^6\rightarrow1s^22s2p^6$. Solid line: time-independent distorted-wave calculations for $1s^22s^22p^6\rightarrow1s^22s^22p^5$ and $1s^22s^22p^6\rightarrow1s^22s2p^6$. Dashed line: LS term-dependent distorted-wave calculation for $1s^22s^22p^6\rightarrow1s^22s^22p^5$ ionization plus standard distorted-wave calculation for $1s^22s^22p^6\rightarrow1s^22s2p^6$ ionization. Solid circles: experimental points of Ref. [26]. ($1.0\ \text{Mb}=1.0\times10^{-18}\ \text{cm}^2$.)

repeated the distorted-wave calculations for the $2p$ subshell ionization cross section for neon using $2p^5kd\ ^1P$ term-dependent Hartree-Fock potentials, while at the same time calculating all other $2p^5kl$ continuua in the same previously used configuration-averaged potential found in Eq. (6). The new $2p$ ionization cross section, combined with the previous $2s$ cross section, is shown in Fig. 3 by a long-dashed line. Although somewhat fortuitous for sure, the now excellent agreement between distorted-wave theory and experiment suggests the need for extending the time-dependent close-coupling method to include a full Hartree-Fock interaction with the remaining core electrons, especially for closed ($l\geqslant1$) subshell systems.

IV. SUMMARY

In this paper, the formulation of the time-dependent close-coupling method has been extended to allow for the calculation of the electron-impact direct ionization of the outer subshell of any atom or ion. The inner subshells are treated using pseudopotentials, while interaction with remaining outer subshell core electrons is handled in a configuration-averaged approximation. In fact, the time-dependent close-coupling method may be used to calculate the direct ionization of the inner subshells of any atom or ion, as long as all excitations to outer open subshells are carefully counted during time propagation of the coupled equations.

For electron-impact ionization of carbon the time-dependent close-coupling results for the $2p$ outer subshell, combined with distorted-wave results for the $2s$ inner subshell, are found to be in reasonable agreement with experimental measurements, especially at lower incident electron

energies. For electron-impact ionization of neon the time-dependent close-coupling results for the $2p$ outer subshell, combined with distorted-wave results for the $2s$ inner subshell, are found to be substantially higher than experimental measurements.

Further LS term-dependent distorted-wave calculations for the $2p$ subshell ionization of neon suggest the need for extending the time-dependent close-coupling method to include a full Hartree-Fock interaction with remaining core electrons, especially for $l \geqslant 1$ closed subshells. The introduction of nonlocal potentials into the time propagation of the two electron radial wave functions will be a major computational challenge. In the meantime, there are many atomic targets for which a configuration-averaged wave-packet approach should yield accurate collision cross sections for both electron and positron scattering.

ACKNOWLEDGMENTS

This work was supported in part by the U.S. Department of Energy. Computational work was carried out at the National Energy Research Supercomputer Center at the Lawrence Berkeley National Laboratory.

[1] S.M. Younger, Phys. Rev. A **22**, 111 (1980).
[2] H. Jakubowicz and D.L. Moores, J. Phys. B **14**, 3733 (1981).
[3] I. Bray and A.T. Stelbovics, Phys. Rev. Lett. **70**, 746 (1993).
[4] D. Kato and S. Watanabe, Phys. Rev. Lett. **74**, 2443 (1995).
[5] K. Bartschat and I. Bray, J. Phys. B **29**, L577 (1996).
[6] M.S. Pindzola and F. Robicheaux, Phys. Rev. A **54**, 2142 (1996).
[7] M.B. Shah, D.S. Elliot, and H.B. Gilbody, J. Phys. B **20**, 3501 (1987).
[8] D.V. Fursa and I. Bray, Phys. Rev. A **52**, 1279 (1995).
[9] E.T. Hudson, K. Bartschat, M.P. Scott, P.G. Burke, and V.M. Burke, J. Phys. B **29**, 5513 (1996).
[10] M.S. Pindzola and F.J. Robicheaux, Phys. Rev. A **61**, 052707 (2000).
[11] R.K. Montague, M.F.A. Harrison, and A.C.H. Smith, J. Phys. B **17**, 3295 (1984).
[12] I. Bray, J. Phys. B **28**, L247 (1995).
[13] K. Bartschat and I. Bray, J. Phys. B **30**, L109 (1997).
[14] M.S. Pindzola, F. Robicheaux, N.R. Badnell, and T.W. Gorczyca, Phys. Rev. A **56**, 1994 (1997).
[15] K. Berrington, J. Pelan, and L. Quigley, J. Phys. B **30**, 4973 (1997).
[16] P.J. Marchalant, K. Bartschat, and I. Bray, J. Phys. B **30**, L435 (1997).
[17] O. Woitke, N. Djuric, G.H. Dunn, M.E. Bannister, A.C.H. Smith, B. Wallbank, N.R. Badnell, and M.S. Pindzola, Phys. Rev. A **58**, 4512 (1998).
[18] D.M. Mitnik, M.S. Pindzola, D.C. Griffin, and N.R. Badnell, J. Phys. B **32**, L479 (1999).
[19] M.P. Scott, H. Teng, and P.G. Burke, J. Phys. B **33**, L63 (2000).
[20] N.R. Badnell, M.S. Pindzola, I. Bray, and D.C. Griffin, J. Phys. B **31**, 911 (1998).
[21] Z. Felfli, K.A. Berrington, and A.Z. Msezane, J. Phys. B **33**, 1263 (2000).
[22] M.S. Pindzola, D.C. Griffin, and C. Bottcher, in *Atomic Processes in Electron-Ion and Ion-Ion Collisions*, Vol. 145 of *NATO Advanced Study Institute Series B: Physics*, edited by F. Brouillard (Plenum Press, New York, 1986), p. 75.
[23] D.H. Sampson, Phys. Rev. A **34**, 986 (1986).
[24] *Atomic Energy Levels I*, edited by C. E. Moore, Natl. Bur. Stand. U.S. NSRDS No. 35 (U.S. GPO, Washington, DC, 1971).
[25] E. Brook, M.F.A. Harrison, and A.C.H. Smith, J. Phys. B **11**, 3115 (1978).
[26] E. Krishnakumar and S.K. Srivastava, J. Phys. B **21**, 1055 (1988).
[27] R.C. Wetzel, F.A. Baiocchi, T.R. Hayes, and R.S. Freund, Phys. Rev. A **35**, 559 (1987).
[28] D.P. Almeida, A.C. Fontes, and C.F.L. Godinho, J. Phys. B **28**, 3335 (1995).
[29] S.M. Younger, Phys. Rev. A **26**, 3177 (1982).
[30] D.C. Griffin, M.S. Pindzola, T.W. Gorczyca, and N.R. Badnell, Phys. Rev. A **51**, 2265 (1995).
[31] M.S. Pindzola, D.C. Griffin, and C. Bottcher, J. Phys. B **16**, L355 (1983).